Heliyon 9 (2023) e13745

Contents lists available at ScienceDirect

Heliyon

journal homepage: www.cell.com/heliyon

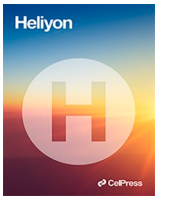

Research article

Improvement of brain–computer interface in motor imagery training through the designing of a dynamic experiment and FBCSP

Chun-Ling Lin [a,*], Liang-Ting Chen [a]

[a] Department of Electrical Engineering, Ming Chi University of Technology, No. 84, Gongzhuan Rd., Taishan Dist., New Taipei City, 243, Taiwan

ARTICLE INFO

Keywords:
Motor imagery
Filter bank common spatial pattern (FBCSP)
Linear discriminant analysis (LDA)

ABSTRACT

Motor imagery (MI) can produce a specific brain pattern when the subject imagines performing a particular action without any actual body movements. According to related previous research, the improvement of the training of MI brainwaves can be adopted by feedback methods in which the analysis of brainwave characteristics is very important. The aim of this study was to improve the subject's MI and the accuracy of classification. In order to ameliorate the accuracy of the MI of the left and right hand, the present study designed static and dynamic visual stimuli in experiments so as to evaluate which one can improve subjects' imagination training. Additionally, the filter bank common spatial pattern (FBCSP) method was used to divide the frequency band range of the brainwaves into multiple segments, following which linear discriminant analysis (LDA) was adopted for classification. The results revealed that the averaged false positive rate (FPR) under FBCSP–LDA in the dynamic MI experiment was the lowest FPR (23.76%). As such, this study suggested that a combination of the dynamic MI experiment and the FBCSP–LDA method improved the overall prediction error rate and ameliorated the performance of the MI brain–computer interface.

1. Introduction

The brain–computer interface (BCI) creates a bridge of communication for humans. BCI can transfer human responses from the brain activity to commands that is used to control external equipment and games [1,2]. Many different types of indices from the brain activity can be adopted to develop a BCI system; the common indices are event-related potential (ERP), event-related desynchronisation (ERD), event-related synchronisation (ERS), and steady-state visually evoked potential (SSVEP), which are derived from the features extracted from the brain activity [3, 4, 5].

Human movement imagination of limbs result in ERD and ERS from the brain activity [6,7]. When a user starts to imagine movements of his/her left and right hands, the mu frequency power (8–13 Hz) and the beta frequency power (13–30 Hz) reveal the ERD condition in the central areas of the brain. Movement imagination applications use these indices from the brain activity to produce control signals [8,9]. However, these indices from the brain activity differ from one individual to another and thus cannot provide a reliable control signal [10,11]. A previous study indicated that 20% of the subjects cannot imagine a movement and produce the related brain activity [10]. This phenomenon is called aphantasia [12].

* Corresponding author.
E-mail address: ginnylin@mail.mcut.edu.tw (C.-L. Lin).

https://doi.org/10.1016/j.heliyon.2023.e13745
Received 9 November 2022; Received in revised form 4 February 2023; Accepted 9 February 2023
Available online 15 February 2023

In order to help subjects to produce and regulate the related brain activity effectively while they imagine the movement, many recent studies have proposed feedback training methods to improve the performance of a motor imagery (MI)-based brain–computer interface (BCI) [13, 14, 15]. Feedback training methods provide users with the information about the brain activity and help them to use effective methods to regulate brain activity and control MI-based BCI accurately [16]. A comparison of the performance of MI between realistic and abstract feedback signals revealed that there is no difference in the training performance of the two different signals [16]. Some of the untrained subjects can even use the MI-based BCI system to quickly learn effective control methods. Kondo et al. suggested that static and dynamic visual stimuli on neurofeedback training affect the different performance of an MI-based BCI on ERD [17]. Bian et al. suggested that the four different MI tasks using the dynamic visual stimuli can induce stronger MI-EEG features and obtain higher classification accuracy than the static stimuli [18]. They hypothesized that the static stimuli of the hand would contradict sensorimotor subjects after the generation of motor commands and produce ERD phenomena [17,18].

Furthermore, common spatial pattern (CSP) is an efficient method to develop the MI-based BCI, because CSP has been used with extracting features in the MI because of its simplicity, high speed, and robustness [19,20]. However, the suitable frequency band is subject-specific for CSP and it is hard to determine [21,22]. Ang et al. proposed filter bank common spatial pattern (FBCSP) to fix the filter band selection problem. FBCSP adopted a set of CSP filters with several time/frequency filters to extract the log–variance features and then concatenated all the features to the classifying tasks by using machine learning. FBCSP can be useful in the case of EEG processes in different frequency bands [22].

Although feedback training methods have both inhibitory and facilitative effects on EEG control, the development of feedback training methods starts with the designed experiment without feedback when the EEG signals are recorded and then uses the last recording EEG data to construct a classifier that can only be used for the next MI-based BCI [23]. Thus, the performance of feedback training methods depends on the initial recording EEG data, and the EEG data may not be distinguished or classified precisely. If the subjects are unfamiliar and inattentive to the BCI system and cannot successfully perform the MI experiment, the feedback signals may frustrate them [14]. If the MI-based BCI system can provide subjects a suitable cue which instruct them how to imagery the hands movement, it can save training time and frustration. Therefore, the development of an effective experimental design and analysis tool is always a major challenge for MI-based BCI system.

Previous studies have reported different ERD phenomena under different static and dynamic visual stimuli [17,18]. A particular property of ERD for the MI task is somatotopic; that is, the MI of a right-hand movement may induce ERD at the contralateral (left) sensorimotor cortex [18]. In addition, Pfurtscheller et al. added ERS as a neuronal condition to improve the classification performance in MI tasks [24]. However, Wolpaw et al. suggested that manipulating the ERD to reflect appropriate mental images is a difficult method to master [25]. Thus, the lack of an in-depth understanding of the physiological mechanisms governing ERD can leave the MI-based BCI system baffled. The problem of enhancing ERD patterns is another attractive area of research. Pichiorri et al. proposed MI-based BCI training to enhance cortical excitability and improve the ERD phenomenon at the end of four weeks. Some studies have attempted to design different experimental paradigms or visual stimuli of MI tasks. Nakayashiki et al. suggested that the kinematic factor in MI tasks can induce ERD significantly [26]. Because ERD can be induced during motor planning, execution, and observation, the experiment can design these factors into MI tasks to enhance ERD. Different ERD enhancements may be caused by different types of visual guidance and stimuli. Pfurtscheller et al. suggested that dynamic hand visual guidance with the moving hand is better than static hand visual guidance [27]. Many previous studies have designed different imagery tasks to induce the ERD and ERS in order to obtain higher classification accuracy [18,20]. Wang et al. proposed the CSP to analyze the spatial patterns of imagined hand and foot movements by means of combining linear discriminant analysis with a view to achieving ERD and readiness potential (RP). The classification accuracies with four optimal channels (C3, CPz, Cz and FCz) were 93.45% and 91.88% for two subjects. Bian et al. designed the four motor imagery tasks with different stimuli and adopted the CSP to extract spatial pattern features. Following this, support vector machines (SVM) were used to classify four kinds of motor imagery and the results showed that the classification accuracy exceeded, or was equal to, 87.5% [18]. Furthermore, they proved that task complexity can enhance alpha ERD phenomena in cognitive tasks and that such complexity can be considered an option for guidance optimization. Some studies have obtained higher classification accuracy (>90%) for left- and right-hand movements imagery tasks [28,29].

However, most previous studies had to analyze multi-channel EEG or required relatively expensive equipment, which easily led to inconvenient recording preparation and complicated calculations. When it comes to designing a practical MI-based BCI, one option is to select fewer channels for application. Furthermore, the question of how to design MI stimuli and guidance to enhance the ERD schema remains truly unanswered [30,31]. The motivation of the current study lay mainly in evaluating whether the static and dynamic visual stimuli of right- and left-hand movement can induce ERD or ERS in the EEG and further evaluate which kinds of ERD or ERS produced by the different visual stimuli can achieve effective classification. We hypothesized that the dynamic visual stimuli of right- and left-hand movement can induce ERD or ERS. If the phenomenon of ERD or ERS was not obvious and would lead to failure of the classification, this paper proposed the FBCSP with linear discriminant analysis (LDA) method to improve the accuracy of classification for a BCI system.

This study attempts to design the static and dynamic visual stimuli of right- and left-hand movement in experiments and to determine whether the different kinds of stimuli have influences on ERD or ERS. In the case of failure of right- and left-hand movements classification using ERD or ERS, classification was assessed and modeled by CSP–LDA and FBCSP–LDA.

2. Methods

2.1. Participants

In all, seven participants (males; mean age: 24 ± 2 years) with normal or corrected-to-normal vision and dominant right hand and from Ming Chi University of Technology were selected for this experiment. All the participants were healthy and had no history of gastrointestinal, cardiovascular, neurological, and/or psychological disorders. The time of experiment was 2–4 pm. Before the experiment, we asked the participants whether they had any BCI experience or not. None of the subjects had any BCI experience. Then, the purpose of the experiment was explained. The participants understood the method of measuring the brainwave program and the motor imagery required by the overall experiment. The Institutional Review Board of Research Ethics Committee National Taiwan University approved the experimental protocol used in this study. Informed consent was obtained from all the participants. Finally, the function of the keyboard was explained because the recording of the brainwave data began as soon as they pressed the button to start the experiment.

2.2. Motor imagery (MI) training experiment

During the experimental session, the participants sat in a comfortable chair in front of a 27" computer monitor. Each trial began with a black background with a cross on the computer monitor for 5 s (a baseline period), followed by the black background for 0.5–0.8 s and visual stimulation for 10 s. Final, the participant rested for 2 s. In order to compare that the performance of the dynamic MI training experiments with that of static MI training experiments, this study designed two types of MI training experiments (Fig. 1) for visual stimulation. The dynamic and static MI training experiments had the right- and left-hand MI stimulations. In the static MI training experiments, the stimulations of right and left hands were a picture which showed an illustration of a left- or right-hand crimping force device. The participants were asked to imagine the picture of their left or right hand crimping the force device. During the imagining process, each subject was asked to imagine that they crimped the force device with their left or right hand from the first-person perspective. The stimulations of the dynamic MI training experiments were in the video format. The simulated video showed that the right or left hand poked the ball and the ball rolled to the opposite hole. The subjects were asked to imagine poking the ball with their left or right hand and then causing the ball to roll in that direction until the ball was pushed into the hole. The complete experiment included 30 trials each of the left- and right-hand MI simulations in the static and dynamic MI training experiments, and the total number of trials was 120. The left- or right-hand MI simulations in the static and dynamic MI training experiments appeared in a random order, and the experimental sessions lasted an hour.

2.3. EEG data acquisition

Continuous EEG was recorded using a NeuroScan system (NuAmps Compumedics Ltd., VIC, Australia). The system contained 32 active electrodes and headcaps with electrode positions according to the extended 10–20 system. EEG signals were sampled at 1 kHz and notch filtered at 60 Hz. The contact impedance between the scalp and the electrode was adjusted to be less than 5 kΩ.

2.4. EEG data analysis

A previous study suggested that the phenomenon of brain imagining ERD and ERS appeared in the motor area and particularly

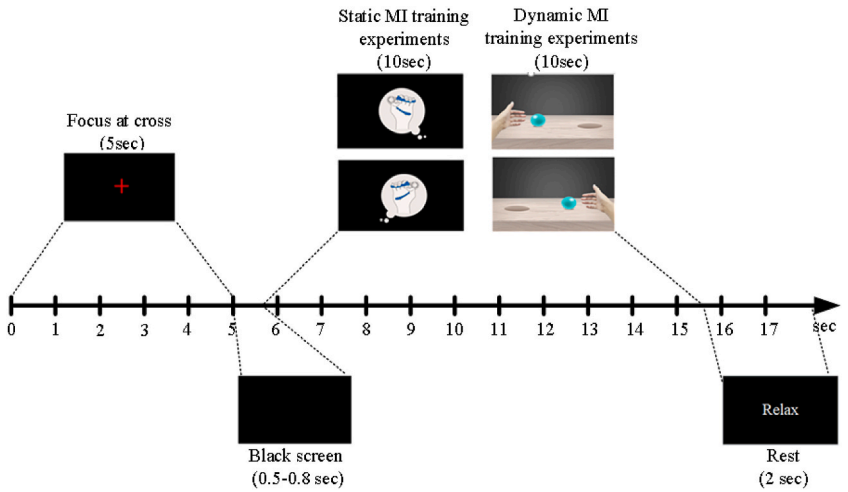

Fig. 1. Designed static and dynamic MI training experiments conducted in this study.

occurred in mu (8–13 Hz) and beta (13–30 Hz) waves when the subject was participating in the hand MI experiment [32,33]. An analysis of this study focused on the location of the motor cortex and the related frequency range of the brain waves. Fig. 2 shows the flowchart of the EEG analysis in this study; it is described in the following subsections.

2.4.1. EEG pre-processing

EEG data were pre-processed in EEGLAB (http://www.sccn.ucsd.edu/eeglab). In order to remove noise including the direct current shifts and the power-line noise in time-series EEG and observe the ERD/ERS condition, that is the mu frequency power (8–13 Hz) and beta frequency power (13–30 Hz) in the central areas of the brain [6,7], a band-pass finite impulse response (FIR) filter between 8 and 30 Hz was applied. Subsequently, data were down-sampled to 250 Hz. Non-physiological artefacts and bad channels in the continuous EEG were rejected by visual inspection to obtain a clean independent component analysis.

On the pruned data, ICA was applied and the EEGLAB plugin EEG Independent Component Labelling was adopted to assist in identifying and rejecting the independent components reflecting stereotypical artefacts such as eye blinks, eye movements, EKG, muscle activity, and line noise [34].

As the experiment was an MI experiment and analyzed the phenomenon of brain imagining ERD and ERS, only the electrodes in the motor area of the cerebral cortex, namely FC3, FCz, FC4, C3, Cz, C4, CP3, CPz, and CP4, were used for further analysis. Single-trial data epochs were extracted from the artefact-corrected time-series EEG data within a time window extending from the 3-s pre-visual stimulus onset to the 10-s post-visual stimulus onset.

2.4.2. ERD and ERS during MI

When humans' senses, cognitive systems, and motor behaviors are in the presence of some external stimulus, the related areas of the cerebral cortex not only produce the potential fluctuations but also automatically change the portion of the EEG associated with the event. This phenomenon is called event-related potential (ERP). At the same time, ERD or ERS occurs [32,35].

The phenomenon of ERD and ERS can be obtained in the EEG data after the following processing [33]:

1. Subtract the mean value of its from each extracted epoch of the EEG.
2. Calculate the energy by taking the square of the amplitude of extracted epoch of the EEG signal.
3. Smoothen the energy of the extracted epoch by using the moving average method (MATLAB Curve Fitting Toolbox, function "smooth").
4. Quantify the percentage of energy drop (or rise) to obtain the ERD (or ERS, Equation (1)):

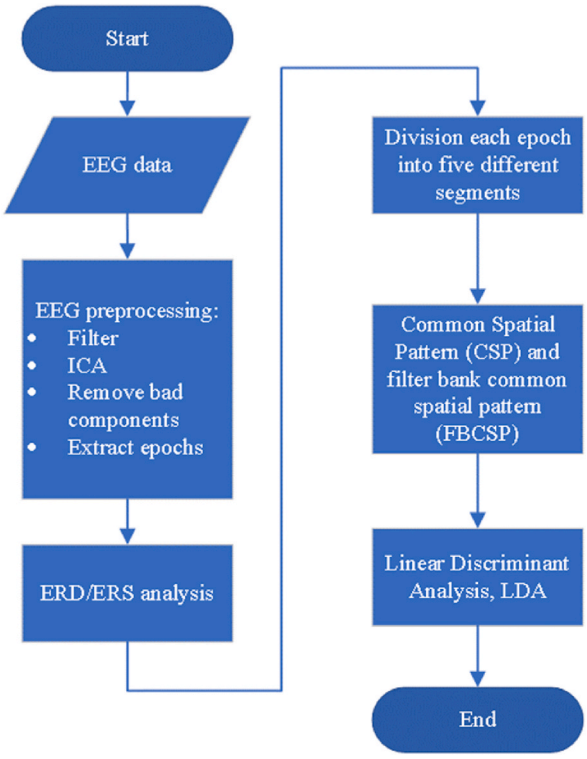

Fig. 2. Flowchart of EEG analysis.

$$ERD = \frac{A - R}{R} \times 100(\%) \quad (1)$$

where A denotes the sum energy of the active cycle which sums the energy with a 1-s window overlapped by 0.25 s and then subtracts the sum energy of the reference cycle R. The reference cycle was obtained at the interval of the 3-s pre-visual stimulus onset.

Although the duration of the cortical activity was short, the amplitude of the potential decreased and increased obviously, as shown in Fig. 3. A standard measure of ERD determined the difference in the signal band power between the baseline before and after the event. The ERD region corresponded to a negative value, i.e. a decrease in power, while the ERS region represented an increase in the signal power [36].

There are certain frequency bands of ERP on both sides of the cerebral hemisphere. When people imagine or perform both right- and left-hand movements, the power of brain waves will be enhanced and weakened. When people imagine the movement of the left hand, not only will the ERD phenomenon occur in the right hemisphere of the brain, but the ERS phenomenon will also occur in the left hemisphere of the brain. Conversely, when people imagine the movement of the right hand, ERD occurs in the left hemisphere of the brain, while ERS occurs in the right hemisphere of the brain [28]. Because of the subjective motor imagination of the brain, the characteristic frequency bands and cerebral cortex correspond to different passive ERD and ERS phenomena. For example, the ERD in the imagination of hand movements basically appears in the 8–12 Hz and 24–30 Hz frequency bands [28]. Therefore, the ERD and ERS phenomena of brain wave signals can be used to evaluate the standard of left- and right-hand motor imagination.

2.4.3. Feature extraction using CSP and FBCSP

CSP is a widely used feature extraction algorithm that uses spatial filters to distinguish two classes for MI-based BCIs [19,20]. The theory of CSP is to adopt a linear transformation to project the multi-channel EEG onto a low-dimensional spatial subspace with a projection matrix. This type of transformation can maximize the variance of two-class signal matrices. That is, CSP diagonalizes the covariance matrices of two classes. The a_{min} of CSP is used to determine the matrix $\boldsymbol{W}$ in order to obtain the spatially filtered signal $\boldsymbol{Z}_j$ of a signal trial EEG $\boldsymbol{E}_j$ as follows (Equation (2)):

$$\boldsymbol{Z}_j = \boldsymbol{W}\boldsymbol{E}_j \quad (2)$$

where $\boldsymbol{E}_j$ denotes the observed single-trial EEG signal from the pass band (8–30 Hz) of the jth trial. $\boldsymbol{W} \in \boldsymbol{R}^{s \times c}$ indicates the CSP projection matrix. The rows of $\boldsymbol{W}$ represent the stationary spatial filters, and the columns of $\boldsymbol{W}^{-1}$ denote the common spatial patterns. The spatially filtered signals $\boldsymbol{Z}_j \in \boldsymbol{R}^{s \times t}$ can maximize the differences in the variance of the two classes of EEG and can be used as the inputs to a classifier. $\boldsymbol{c}$ indicates the number of channels. t represents the number of time samples, and $j = 1 \ldots n$, where n refers to the number of trials of training sets. Furthermore, s denotes the number of CSP projections, where $s = 2 \times e \times 1(\textit{frequency bands}) \times 2(\textit{clasess})$. In order to select the CSP features for the training model, $e = 2$ eigenvectors from the top and the bottom of the eigenvalue spectrum were chosen as the features [22].

However, the performance of CSP was dependent on its operational frequency band. For the CSP, Dornhege et al. suggested setting a broad frequency range or manually selecting a subject specific frequency range [21,22]. Recently, an alternative approach to FBCSP was proposed to solve the problem of manually selecting a specific frequency band for the CSP algorithm [37]. FBCSP selects the optimal filter band to extract EEG features by estimating the mutual information among the CSP features in several fixed filter bands. FBCSP has four processing steps that include signal processing and machine learning.

A. Different band-pass filters that decomposed EEG into multiple frequency bands using the Chebyshev Type II filter are used in this step. In this study, a total of eight band-pass filters were designed, namely 8–12 Hz, 14–18 Hz, 16–20 Hz, 18–22 Hz, 20–24 Hz,

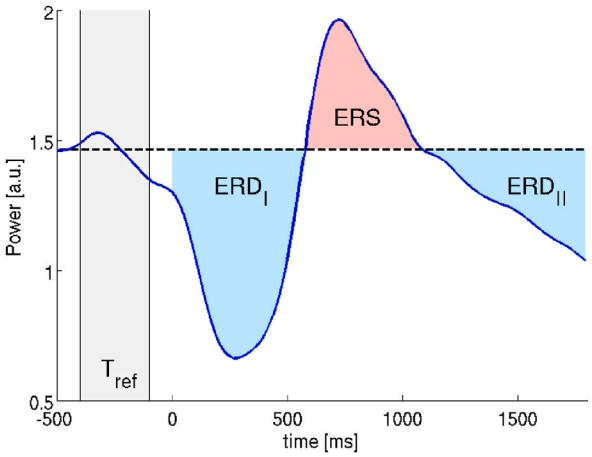

Fig. 3. Phenomenon of ERD and ERS [36].

22–26 Hz, 24–28 Hz, and 26–30 Hz, which denote the covering ranges of the mu and beta rhythms to produce the eight filtered signals.

B. The CSP algorithm used the eight filtered signals and generated the spatially filtered signals individually.
C. For 8 frequency bands of the CSP algorithm, the feature was selected according to the eigenvectors from the top and the bottom of the eigenvalue spectrum. Here, $s = 2 \times e \times 8(\textit{frequency bands}) \times 2(\textit{clasess})$.
D. Finally, LDA was adopted to classify these features into two classes on the basis of the left versus right hand MI tasks.

Although the characteristics of brain waves could be identified from the abovementioned phenomena of ERD and ERS, and the methods of CSP and FBCSP had their own advantages and disadvantages, as listed in Table 1.

A comparison of all these advantages and disadvantages revealed that FBCSP was the most effective improvement method of the three. This study attempted to determine the discriminatively suitable ERD/ERS features from multiple frequency bands of mu and beta and the effective imagery time window by using the comment feature selection algorithms, namely CSP and FBCSP, designed in BCILAB [38] (MATLAB toolbox and EEGLAB plugin, https://github.com/sccn/BCILAB). The interval of the extracted epoch was from the 3-s pre-visual stimulus onset to the 10-s post-visual stimulus onset. Because the motor imagination of each subject was not consistent, this study divided each epoch into five different segments, namely 2−9 s, 3−9 s, 4−9 s, 5−9 s, and 6−9 s, as the post-visual stimulus onset to determine the subject's best MI segment. Then, the five different segments imported CSP and FBCSP, respectively, through BCILAB.

2.4.4. Performance evaluation

This study adopted LDA [39] to classify the EEG data into two classes on the basis of the CSP and FBCSP features from left versus right hand MI tasks. The study adopted the 10-fold cross-validation method to estimate the optimal parameters in the model and to avoid overfitting problems in the classifiers for the training data [40]. For each subject's data, this study divided all the MI trials into k = 10 parts of equal size; nine of them formed the training set to evaluate the classification performance, and the remaining part for the testing set for determining the prediction accuracy. This study proposed two combination methods (CSP–LDA and FBCSP–LDA) and applied these methods to five different segments (2−9 s, 3−9 s, 4−9 s, 5−9 s, and 6−9 s). This study adopted the false positive rate (FPR, Equation (3)) to measure the performance of the classification models.

$$FPR = 1 - Spcificity = \frac{TN}{TN + FP} \tag{3}$$

where FP denotes the number of false positives and TN indicates the number of true negatives.

Because the 10-fold cross-validation method was repeated for 10 times, the performance of the proposed method was estimated by calculating the average of the 10 performance results of the classification, obtained for 10 testing sets.

In addition, this study adopted a particular element – namely accuracy (Equation (4)) – to compare the performance of the proposed method with other previous studies:

$$Accuracy = \frac{TP + TN}{TN + TP + FP + FN} \tag{4}$$

where TP denotes the number of true positives and TN indicates the number of true negatives.

3. Results

3.1. ERD/ERS during imagination of right- and left-hand movements

Fig. 4 shows the ERD/ERS around the channels of C3 and C4 from two subjects during the imagination of right- and left-hand movements in the static and dynamic MI experiments. A comparison of the difference between C3 and C4 of the two subjects revealed that Subject A exhibited an obvious difference between C3 and C4. However, the results of this study were not completely consistent with the theory [28,41] and suggested that the brain wave measured by the C4 electrode was lower than that by C3 when imagining the movement of the left hand. Conversely, the brain wave measured by the C3 electrode was lower than that by C4 when imagining the movement of the right hand. Moreover, only subject A during the imagination of right-hand movements in the static MI experiments (Fig. 4 (a) and (b)) and during the imagination of left-hand movements in the dynamic MI experiments (Fig. 4 (c) and (d)) had obvious ERD/ERS.

Table 1
Advantages and disadvantages of brainwave feature methods.

Method	Advantages	Disadvantages
ERD/ERS	Makes it easy to observe the rise and fall of EEG power.	Different results for different subjects make the phenomenon difficult to determine.
CSP	Makes the brainwave characteristic phenomenon obvious.	Only a single frequency band can be analyzed.
FBCSP	Divides brainwave data into multiple frequency segments and reduces the computational complexity.	Requires a large structure and long operation time.

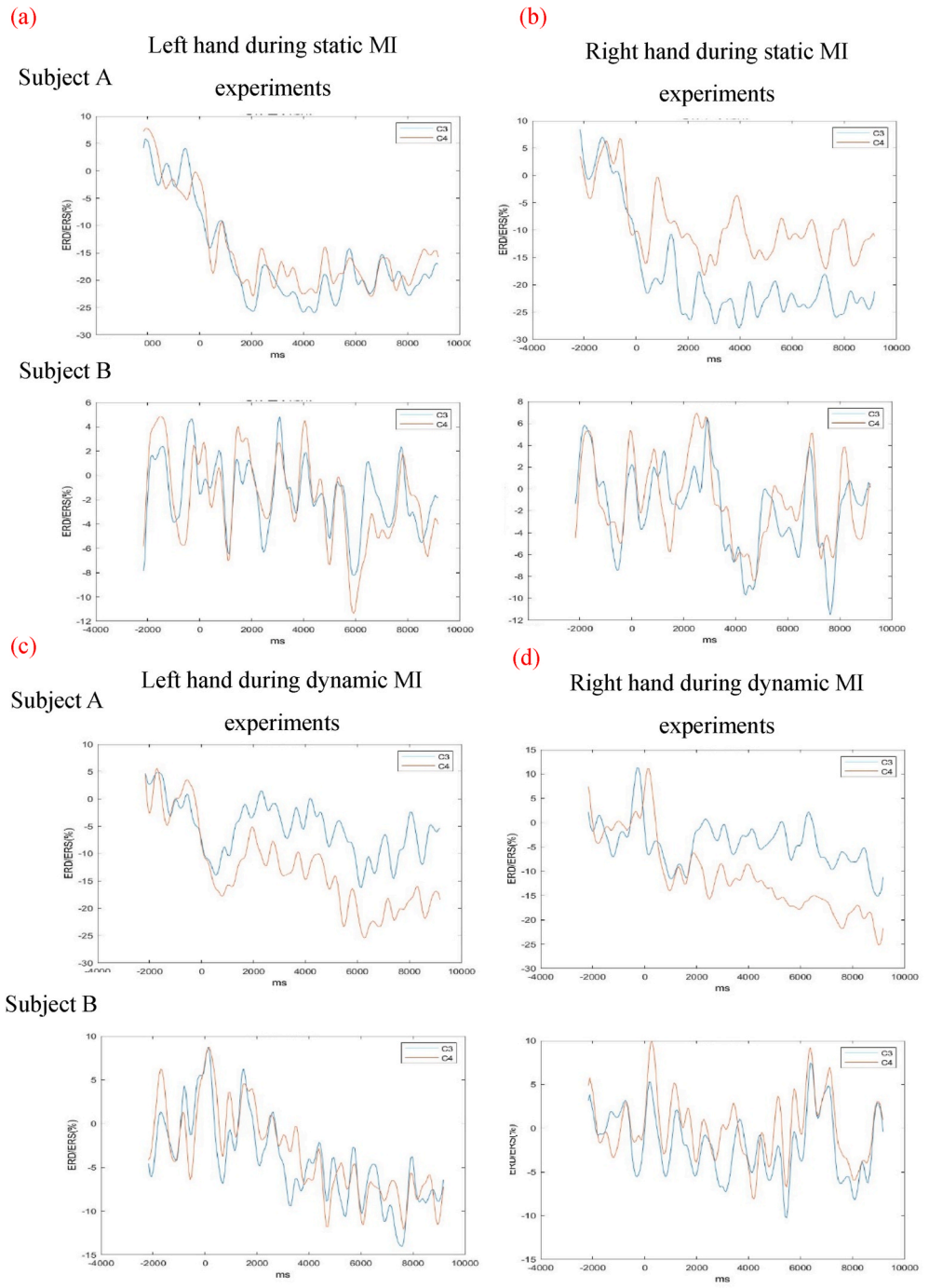

Fig. 4. ERD/ERS from two subjects during imagination of right- and left-hand movements in the static and dynamic MI experiments. ERD/ERS around the channels of C3 and C4 from two subjects during the imagination of (a) left- and (b) right-hand movements in the static MI experiments. ERD/ERS around channels of C3 and C4 from two subjects during the imagination of (c) left- and (d) right-hand movements in the dynamic MI experiments.

This study adopted the Wilcoxon signed rank [42] to test the difference in ERD/ERS among seven subjects (blue point in Fig. 5 ($p <$ 0.05)). Fig. 5 also shows the mean and standard deviation (std) of ERD/ERS across seven subjects during the imagination of right- and left-hand movements in the static and dynamic MI experiments. The results showed that there were no significant differences between C3 and C4 before the 0-s mark, which was the baseline section. Thus, the results indicated that the brain activations in the baseline section were all under the same baseline. However, ERD/ERS during the imagination of right-hand movements in the static MI

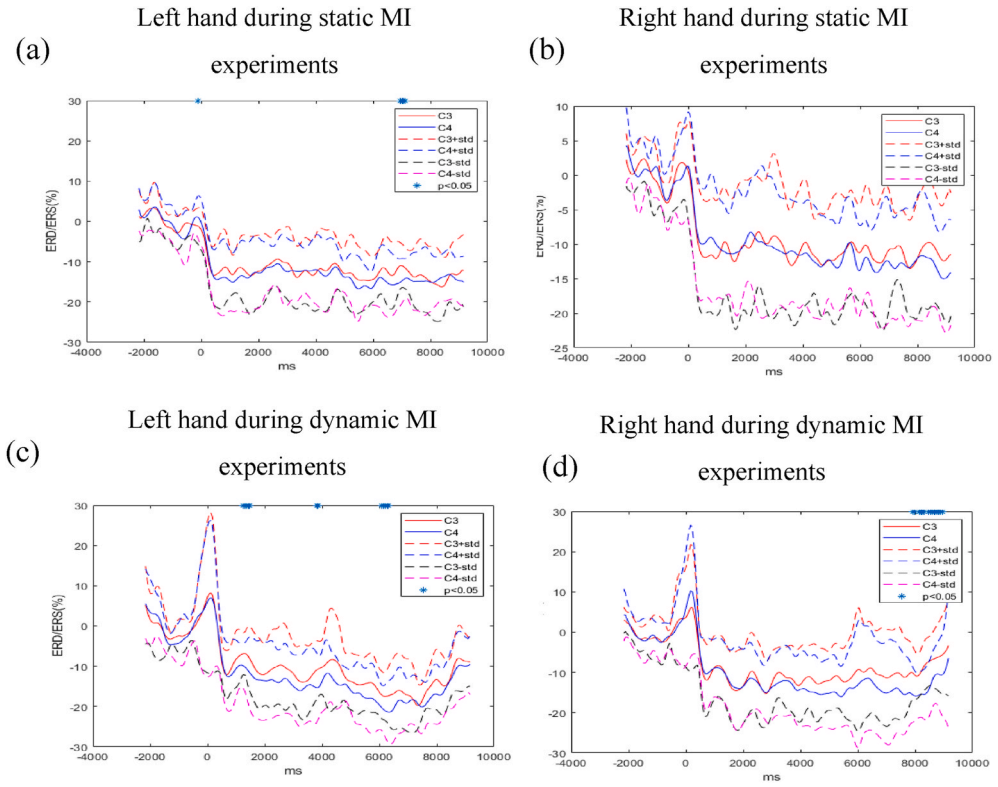

Fig. 5. Mean and standard deviation (std) of ERD/ERS across seven subjects during imagination of (a) left- and (b) right-hand movements in the static MI experiments. Mean and standard deviation (std) of ERD/ERS across seven subjects during imagination of (c) left- and (d) right-hand movements in the dynamic MI experiments. The blue point indicates significant differences between C3 and C4 ($p < 0.05$).

experiments had no significant differences between C3 and C4 (Fig. 5(b)). ERD/ERS during the imagination of left-hand movements in the static and dynamic MI experiments exhibited non-continuous significant differences between C3 and C4 (Fig. 5(a) and (c)). Fig. 5 (d) shows the continuous significant differences between C3 and C4, but this phenomenon was abnormal; it has also been reported in [43]. Choi et al. suggested that distinctive classification did not exist in each frequency for ERD in the alpha band or ERS in the beta band during the MI experiment, indicating that there were no significant differences in ERD/ERS between C3 and C4 [44]. Even when the experimental design was changed to dynamic scene cues in this study, no effective identification feature was obtained from the ERD/ERS phenomenon.

According to the discussion of previous studies [45–47], there is considerable inter- and intra-subject variability in ERD/ERS during MI tasks. The relationship between the variability of ERD and ERS during MI tasks and the performances of the MI-based BCI system is

Table 2
FPR of different segments between CSP–LDA and FBCSP–LDA in a static MI experiment. Boldface indicates the best imaginary time period for each subject.

Different segments Subject		2–9 s	3–9 s	4–9 s	5–9 s	6–9 s
A	CSP–LDA	**20.33%**	23.67%	32%	28.67%	30.33%
	FBCSP–LDA	**17%**	25.33%	28.33%	30%	27%
B	CSP–LDA	58.33%	**45%**	66.67%	56.67%	48.33%
	FBCSP–LDA	**53.33%**	63.33%	71.67%	71.67%	68.33%
C	CSP–LDA	45%	45%	43.33%	**41.67%**	50%
	FBCSP–LDA	60%	56.67%	**53.33%**	61.67%	61.67%
D	CSP–LDA	**40%**	45%	52%	44%	53.33%
	FBCSP–LDA	54.67%	**47.67%**	52.67%	49%	60.67%
E	CSP–LDA	**41.67%**	45%	45%	50%	56.67%
	FBCSP–LDA	41.67%	**36.67%**	46.67%	40%	41.67%
F	CSP–LDA	22.67%	**21.33%**	26.67%	40%	40.33%
	FBCSP–LDA	**21.67%**	25.67%	36.33%	42.67%	27.33%
G	CSP–LDA	56.67%	56.67%	56.67%	**51%**	55.33%
	FBCSP–LDA	38.33%	42.33%	43.67%	51%	**37.67%**

still not well understood. Many previous studies have averaged ERD or ERS patterns across trials and possibly across all subjects to observe the ERD or ERS phenomena. Thus, an analysis of the inter- and intra-subjects in ERD/ERS and their variability throughout the experiment has been largely neglected in most studies. In order to develop an effective MI-based BCI system, we believe that it is very important to understand the intra and inter-individual variability of ERD/ERS during BCI. In further work, this study will further analyze the existing variability both across all the trials of each subject and across all the trials of an experiment. The purpose of this will be to explore the different motor imagination conditions of different subjects. Depending on the results of further work, it may be possible to revise the dynamic MI experiment in this study.

3.2. Classification results from two combination methods (CSP–LDA and FBCSP–LDA)

This study proposed two combination methods (CSP–LDA and FBCSP–LDA) and applied these methods for five different segments (2−9 s, 3−9 s, 4−9 s, 5−9 s, and 6−9 s). Then, the study adopted the 10-fold cross-validation method to check the performance of CSP–LDA and FBCSP–LDA. Table 2 shows the FPR of different segments for CSP–LDA and FBCSP–LDA in a static MI experiment and the best imaginary time period for each subject which had the lowest FPR, and Table 3 shows the lowest FPR from each subject among the five segments for CSP–LDA and FBCSP–LDA and the averaged FRP for CSP–LDA and FBCSP–LDA. The averaged FRP for CSP–LDA and FBCSP–LDA was 37.28% and 38.19%, respectively. There were two subjects (A and E) with the lowest FPR for CSP–LDA and FBCSP–LDA among the seven subjects.

Table 4 shows the FPR of different segments for CSP–LDA and FBCSP–LDA in a dynamic MI experiment, and Table 5 shows the lowest FPR for each subject among the five segments for CSP–LDA and FBCSP–LDA and the averaged FRP for CSP–LDA and FBCSP–LDA. A comparison of the results of Tables 4 and 5 with those of Tables 2 and 3 revealed that the averaged FPR for FBCSP–LDA in the dynamic MI experiment was 23.76%, which was lower than that for CSP–LDA in the same experiment (40.90%) and was better than that for the same method in the static MI experiment (38.19%). In addition, the FPR of all the subjects decreased, and the FPR of subjects A and F improved. These results showed that the FPR of each subject in the cases of CSP–LDA and FBCSP–LDA in the static MI experiment were higher than those in the dynamic MI experiment. Thus, this study suggested that a combination of the dynamic MI experiment with the FBCSP–LDA method improved the overall prediction error rate and improved the performance of MI BCI.

This study also adopted the leave-one-subject-out cross-validation (LOSO CV) [48] to test the performance of FBCSP–LDA in the dynamic MI experiment. That is, the data from one subject were the testing data, and the rest were the training data. However, the results showed that FPR in any imaginary segment was not ideal, and the average FPR rate was higher than 40%. Thus, the study suggested that imaginary data of different subjects could not be used as training data and FBCSP–LDA must adopt the training data and the testing data from the same subject. This may be a result of the small amount of knowledge regarding variability of cerebral motor patterns from FBCSP [49,50]. As a future work path, this study plans to extend such analyses, including the temporal and spatial variability of event-related spectral perturbation (ERSP), while also taking into account different machine learning models.

The present study combined the dynamic MI experiment with the FBCSP–LDA method and adopted the 10-fold cross-validation approach to assess the performance of the proposed method. The results show that the averaged FPR was 23.76%, and average accuracy was 73.23%. Table 6 illustrates the comparison of the proposed method with previous methods of classification of left- and right-hand motor imagination. The results listed in Table 6 show that, if the designed MI experiment was dynamic, then the feature extraction method and classification method could adopt the simple FBCSP–LDA method, and the accuracy of the classification of the left- and right-hand motor imagination can be close to that of complex algorithms.

4. Conclusion

The aim of this study was to design a dynamic MI experiment to induce motor-imagery electroencephalogram signals (MI-EEG) and then adopt the filter bank common spatial pattern (FBCSP) with linear discriminant analysis (LDA) method to improve the performance of an MI-based BCI system. According to the collection of brain waves from seven healthy subjects in different experiments, the ERD/ERS phenomenon were variable and no distinctive classification was found. The results of FPRs of CSP–LDA and FBCSP–LDA in different experiments showed that the averaged FPR for FBCSP–LDA in the dynamic MI experiment was the lowest FPR (23.76%). Thus, this study suggested that a combination of the dynamic MI experiment with the FBCSP–LDA method improved the overall prediction error rate and improved the performance of MI BCI.

Table 3
FPR of seven subjects in static MI experiment. Boldface indicates the lowest two FPRs under CSP–LDA and FBCSP-–LDA.

Subject	CSP–LDA FPR (%)	FBCSP–LDA FPR (%)
A	**20.33**	**17**
B	45	53.33
C	41.67	53.33
D	40	47.67
E	41.67	36.67
F	**21.33**	**21.67**
G	51	37.67
Average	37.28	38.19

Table 4
FPR of different segments for CSP–LDA and FBCSP–LDA in a dynamic MI experiment. Boldface indicates the best imaginary time period for each subject.

Different segments	Subject	2–9 s	3–9 s	4–9 s	5–9 s	6–9 s
A	CSP–LDA	**42.33%**	48.67%	54.33%	47.67%	48.67%
	FBCSP–LDA	17%	**16.67%**	20%	22%	20.33%
B	CSP–LDA	47%	49%	52.33%	**38.67%**	42%
	FBCSP–LDA	31%	25.33%	32%	**20%**	37.67%
C	CSP–LDA	45.33%	47.33%	41.67%	41.67%	**36.33%**
	FBCSP–LDA	**19.33%**	44.67%	37%	47%	41%
D	CSP–LDA	51.67%	55%	56.67%	43.33%	**38.33%**
	FBCSP–LDA	55%	51.67%	46.67%	38.33%	**36.67%**
E	CSP–LDA	49.33%	53%	51.33%	**47.67%**	49.33%
	FBCSP–LDA	41.33%	39.33%	36%	**32.33%**	47.67%
F	CSP–LDA	41.67%	**38.33%**	46.67%	48.33%	45%
	FBCSP–LDA	11.67%	11.67%	**5%**	8.33%	11.67%
G	CSP–LDA	55.33%	50.67%	**44.67%**	**44.67%**	45.67%
	FBCSP–LDA	37.67%	**36.33%**	41%	43%	40%

Table 5
FPR of seven subjects in a dynamic MI experiment. Boldface indicates lowest two FPR for CSP–LDA and FBCSP–LDA.

Subject	CSP–LDA FPR (%)	FBCSP–LDA FPR (%)
A	42.33	**16.67**
B	38.67	20
C	36.33	19.33
D	38.33	36.67
E	47.67	32.33
F	38.33	**5**
G	44.67	36.33
Average	**40.90**	**23.76**

Table 6
Performance comparison of the proposed method with previous works.

Study	Methods	Accuracy
Pramod et al. [51]	Multivariate empirical mode decomposition (MEMD) using subject independent BCI (MEMD-SI-BCI) with LDA	72.92%
Mohammad et al. [52]	Power spectral density (PSD) with LDA classifier	74%
Kaya and Saritas [53]	Power Spectral Density (PSD) with welch method, Wavelet Decomposition (WD), Empirical Mode Decomposition (EMD) and Hilbert-Huang Transform (HHT) with Artificial Neural Network (ANN)	74.5%
Proposed method	Dynamic MI experiment with the FBCSP–LDA	73.24%

There exist two major limitations in this study which could be addressed in future research. First, the effect estimates in ERD and ERS under static and dynamic visual stimuli and models (CSP–LDA and FBCSP–LDA) are based on the sufficient sample size for statistical measurements. However, only seven participants from Ming Chi University of Technology were selected for this experiment. Thus, we can increase the number of participants for statistical measurements. Second, we can propose real-time online testing of the MI-based BCI system. Thus, in the future, we will further analyze the existing variability across both all of the trials of each subject and all of the trials of an experiment to explore the different motor imagination conditions of different subjects.

Author contribution statement

Chun-Ling Lin: Conceived and designed the experiments; Analyzed and interpreted the data; Contributed reagents, materials, analysis tools or data; Wrote the paper. Liang-Ting Chen: Conceived and designed the experiments; Performed the experiments; Analyzed and interpreted the data; Contributed reagents, materials, analysis tools or data; Wrote the paper.

Funding statement

This work was supported by Aiming for the Talent Cultivation Project, Ministry of Education of Taiwan; and National Science and Technology Council of Taiwan [MOST 111-2221-E–131-030].

Data availability statement

The authors do not have permission to share data.

Declaration of interest's statement

The authors declare no conflict of interest.

References

[1] J.R. Wolpaw, N. Birbaumer, D.J. McFarland, G. Pfurtscheller, T.M. Vaughan, Brain–computer interfaces for communication and control, Clin. Neurophysiol. 113 (2002) 767–791.
[2] J. Jin, B.Z. Allison, E.W. Sellers, C. Brunner, P. Horki, X. Wang, et al., An adaptive P300-based control system, J. Neural. Eng. 8 (2011), 036006.
[3] X. Chen, Y. Wang, M. Nakanishi, X. Gao, T.-P. Jung, S. Gao, High-speed spelling with a noninvasive brain–computer interface, Proc. Natl. Acad. Sci. USA 112 (2015) E6058–E6067.
[4] Y. Li, J. Pan, J. Long, T. Yu, F. Wang, Z. Yu, et al., Multimodal BCIs: target detection, multidimensional control, and awareness evaluation in patients with disorder of consciousness, Proc. IEEE 104 (2015) 332–352.
[5] D. Zhang, B. Hong, X. Gao, S. Gao, B. Roder, Exploring steady-state visual evoked potentials as an index for intermodal and crossmodal spatial attention, Psychophysiology 48 (2011) 665–675.
[6] G. Pfurtscheller, C. Neuper, D. Flotzinger, M. Pregenzer, EEG-based discrimination between imagination of right and left hand movement, Electroencephalogr. Clin. Neurophysiol. 103 (1997) 642–651.
[7] J. Esther, T. UmmalSarbaBegum, Exploration of EEG based classification using imagined motor movements, Mater. Today Proc. (2021).
[8] B. Xia, Q. Zhang, H. Xie, J. Li, A Neurofeedback Training Paradigm for Motor Imagery Based Brain-Computer Interface. The 2012 International Joint Conference on Neural Networks (IJCNN), IEEE, 2012, pp. 1–4.
[9] R. Zhang, Y. Li, Y. Yan, H. Zhang, S. Wu, T. Yu, et al., Control of a wheelchair in an indoor environment based on a brain–computer interface and automated navigation, IEEE Trans. Neural Syst. Rehabil. Eng. 24 (2015) 128–139.
[10] B. Blankertz, C. Sannelli, S. Halder, E.M. Hammer, A. Kubler, K.-R. Muller, et al., Neurophysiological predictor of SMR-based BCI performance, Neuroimage 51 (2010) 1303–1309.
[11] B. Blankertz, F. Losch, M. Krauledat, G. Dornhege, G. Curio, K.-R. Muller, The berlin brain-computer interface: accurate performance from first-session in BCI-naive subjects, IEEE Trans. Biomed. Eng. 55 (2008) 2452–2462.
[12] T. Kaufmann, S.M. Schulz, A. Koblitz, G. Renner, C. Wessig, A. Kubler, Face stimuli effectively prevent brain–computer interface inefficiency in patients with neurodegenerative disease, Clin. Neurophysiol. 124 (2013) 893–900.
[13] M. Gonzalez-Franco, P. Yuan, D. Zhang, B. Hong, S. Gao, Motor imagery based brain-computer interface: a study of the effect of positive and negative feedback, in: Annual International Conference of the IEEE Engineering in Medicine and Biology Society, IEEE, 2011, pp. 6323–6326.
[14] T. Yu, J. Xiao, F. Wang, R. Zhang, Z. Gu, A. Cichocki, et al., Enhanced motor imagery training using a hybrid BCI with feedback, IEEE (Inst. Electr. Electron. Eng.) Trans. Biomed. Eng. 62 (2015) 1706–1717.
[15] J.W. Choi, S. Huh, S. Jo, Improving performance in motor imagery BCI-based control applications via virtually embodied feedback, Comput. Biol. Med. 127 (2020), 104079.
[16] C. Neuper, R. Scherer, S. Wriessnegger, G. Pfurtscheller, Motor imagery and action observation: modulation of sensorimotor brain rhythms during mental control of a brain–computer interface, Clin. Neurophysiol. 120 (2009) 239–247.
[17] T. Kondo, M. Saeki, Y. Hayashi, K. Nakayashiki, Y. Takata, Effect of instructive visual stimuli on neurofeedback training for motor imagery-based brain–computer interface, Hum. Mov. Sci. 43 (2015) 239–249.
[18] Y. Bian, H. Qi, L. Zhao, D. Ming, T. Guo, X. Fu, Improvements in event-related desynchronization and classification performance of motor imagery using instructive dynamic guidance and complex tasks, Comput. Biol. Med. 96 (2018) 266–273.
[19] H. Lu, H.-L. Eng, C. Guan, K.N. Plataniotis, A.N. Venetsanopoulos, Regularized common spatial pattern with aggregation for EEG classification in small-sample setting, IEEE Trans. Biomed. Eng. 57 (2010) 2936–2946.
[20] Y. Wang, S. Gao, X. Gao, Common spatial pattern method for channel selelction in motor imagery based brain-computer interface, in: IEEE Engineering in Medicine and Biology 27th Annual Conference, IEEE, 2005, pp. 5392–5395.
[21] G. Dornhege, B. Blankertz, M. Krauledat, F. Losch, G. Curio, K.-R. Muller, Combined optimization of spatial and temporal filters for improving brain-computer interfacing, IEEE Trans. Biomed. Eng. 53 (2006) 2274–2281.
[22] M. Tariq, P.M. Trivailo, M. Simic, Classification of left and right foot kinaesthetic motor imagery using common spatial pattern, Biomedical Physics & Engineering Express 6 (2019), 015008.
[23] D.J. McFarland, L.M. McCane, J.R. Wolpaw, EEG-based communication and control: short-term role of feedback, IEEE Trans. Rehabil. Eng. 6 (1998) 7–11.
[24] G. Pfurtscheller, C. Brunner, A. Schlogl, F.L. Da Silva, Mu rhythm (de) synchronization and EEG single-trial classification of different motor imagery tasks, Neuroimage 31 (2006) 153–159.
[25] J.R. Wolpaw, Brain-computer interfaces (BCIs) for communication and control, in: Proceedings of the 9th International ACM SIGACCESS Conference on Computers and Accessibility, 2007, pp. 1–2.
[26] K. Nakayashiki, M. Saeki, Y. Takata, Y. Hayashi, T. Kondo, Modulation of event-related desynchronization during kinematic and kinetic hand movements, J. NeuroEng. Rehabil. 11 (2014) 1–9.
[27] G. Pfurtscheller, R. Scherer, R. Leeb, C. Keinrath, C. Neuper, F. Lee, et al., Viewing moving objects in virtual reality can change the dynamics of sensorimotor EEG rhythms, Presence 16 (2007) 111–118.
[28] H. Ramoser, J. Muller-Gerking, G. Pfurtscheller, Optimal spatial filtering of single trial EEG during imagined hand movement, IEEE Trans. Rehabil. Eng. 8 (2000) 441–446.
[29] G. Dornhege, B. Blankertz, G. Curio, K.-R. Muller, Boosting bit rates in noninvasive EEG single-trial classifications by feature combination and multiclass paradigms, IEEE Trans. Biomed. Eng. 51 (2004) 993–1002.
[30] C. Jeunet, E. Jahanpour, F. Lotte, Why standard brain-computer interface (BCI) training protocols should be changed: an experimental study, J. Neural. Eng. 13 (2016), 036024.
[31] S. Rimbert, D. Trocellier, F. Lotte, Is Event-Related Desynchronization variability correlated with BCI performance? 2022, in: IEEE International Conference on Metrology for Extended Reality, Artificial Intelligence and Neural Engineering (MetroXRAINE), IEEE, 2022, pp. 163–168.
[32] S. Duan, T. Xu, W. Zhuang, D. Mao, The feature extraction of ERD/ERS signals based on the wavelet package and ICA, in: Proceeding of the 11th World Congress on Intelligent Control and Automation, IEEE, 2014, pp. 5621–5625.
[33] -C. Lo Y-CwaP, Investigation of the ERD Approach for BCI System Design, 2003.
[34] J. Ju, H. Zheng, C. Li, X. Li, H. Liu, T. Liu, AGCNNs: attention-guided convolutional neural networks for infrared head pose estimation in assisted driving system, Infrared Phys. Technol. 123 (2022), 104146.
[35] G. Pfurtscheller, Functional brain imaging based on ERD/ERS, Vis. Res. 41 (2001) 1257–1260.

[36] S. Lemm, K.-R. Muller, G. Curio, A generalized framework for quantifying the dynamics of EEG event-related desynchronization, PLoS Comput. Biol. 5 (2009), e1000453.
[37] K.K. Ang, Z.Y. Chin, H. Zhang, C. Guan, Filter bank common spatial pattern (FBCSP) in brain-computer interface, in: IEEE International Joint Conference on Neural Networks (IEEE World Congress on Computational Intelligence), IEEE, 2008, pp. 2390–2397.
[38] C.A. Kothe, S. Makeig, BCILAB: a platform for brain–computer interface development, J. Neural. Eng. 10 (2013), 056014.
[39] F. Lotte, L. Bougrain, A. Cichocki, M. Clerc, M. Congedo, A. Rakotomamonjy, et al., A review of classification algorithms for EEG-based brain–computer interfaces: a 10 year update, J. Neural. Eng. 15 (2018), 031005.
[40] A.B. Buriro, B. Ahmed, G. Baloch, J. Ahmed, R. Shoorangiz, S.J. Weddell, et al., Classification of alcoholic EEG signals using wavelet scattering transform-based features, Comput. Biol. Med. 139 (2021), 104969.
[41] A. Broniec, Analysis of EEG signal by flicker-noise spectroscopy: identification of right-/left-hand movement imagination, Med. Biol. Eng. Comput. 54 (2016) 1935–1947.
[42] H.-T. Hsu, W.-K. Lee, K.-K. Shyu, T.-K. Yeh, C.-Y. Chang, P.-L. Lee, Analyses of EEG oscillatory activities during slow and fast repetitive movements using Holo-Hilbert spectral analysis, IEEE Trans. Neural Syst. Rehabil. Eng. 26 (2018) 1659–1668.
[43] H. Xie, D. Xiao, B. Xia, J. Li, H. Yang, Q. Zhang, The research for the correlation between ERD/ERS and CSP, in: Seventh International Conference on Natural Computation, IEEE, 2011, pp. 1872–1876.
[44] M.-H. Choi, B. Kim, H.-S. Kim, S.-Y. Gim, W.-R. Kim, S.-C. Chung, Perceptual threshold level for the tactile stimulation and response features of ERD/ERS-based specific indices upon changes in high-frequency vibrations, Front. Hum. Neurosci. 11 (2017) 207.
[45] S.C. Wriessnegger, G.R. Muller-Putz, C. Brunner, A.I. Sburlea, Inter-and intra-individual variability in brain oscillations during sports motor imagery, Front. Hum. Neurosci. 14 (2020), 576241.
[46] B.E. Kilavik, M. Zaepffel, A. Brovelli, W.A. MacKay, A. Riehle, The ups and downs of beta oscillations in sensorimotor cortex, Exp. Neurol. 245 (2013) 15–26.
[47] S. Saha, M. Baumert, Intra-and inter-subject variability in EEG-based sensorimotor brain computer interface: a review, Front. Comput. Neurosci. 13 (2020) 87.
[48] M.P. Pauli, C. Pohl, M. Golz, Balanced leave-one-subject-out cross-validation for microsleep classification, Current Directions in Biomedical Engineering 7 (2021) 147–150.
[49] B.Z. Allison, C. Neuper, Could Anyone Use a BCI? Brain-Computer Interfaces, Springer, 2010, pp. 35–54.
[50] S. Hetu, M. Gregoire, A. Saimpont, M.-P. Coll, F. Eugene, P.-E. Michon, et al., The neural network of motor imagery: an ALE meta-analysis, Neurosci. Biobehav. Rev. 37 (2013) 930–949.
[51] P. Gaur, R.B. Pachori, H. Wang, G. Prasad, A multivariate empirical mode decomposition based filtering for subject independent BCI, in: 27th Irish Signals and Systems Conference (ISSC), IEEE, 2016, pp. 1–7.
[52] M.N. Alam, M.I. Ibrahimy, S. Motakabber, Feature extraction of EEG signal by power spectral density for motor imagery based BCI, in: 8th International Conference on Computer and Communication Engineering (ICCCE), IEEE, 2021, pp. 234–237.
[53] E. Kaya, I. Saritas, Motor imagery BCI classification with frequency and time-frequency features by using different dimensions of the feature space using autoencoders, Intelligent Methods In Engineering Sciences 1 (2022) 8–12.